A New Algorithm for Optimizing TV-Based PolSAR Despeckling Model

Xiangli Nie, *Member, IEEE*, Bo Zhang, *Member, IEEE*, Yunjin Chen, and Hong Qiao, *Senior Member, IEEE*

***Abstract*—The Wishart fidelity and total variation (TV) based variational model (WisTV) with the positive definite (PD) constraint has shown to be effective for the whole PolSAR covariance data speckle reduction. However, the existing algorithms for solving the WisTV model only give approximation solutions by projecting the results onto the set of PD matrices, and their parameters depend strongly on the data. The purpose of this letter is to propose a new optimization algorithm to address the issues. To keep the uniformity of the parameters for different PolSAR data, a sigmoid function-based normalization method is designed, which ensures the applicability of the WisTV model for the normalized data. By using the orthogonal decomposition of the PD variables, the WisTV model is converted into an unconstrained optimization problem which is further transformed into a multivariable problem based on the equivalent representations of the trace and logdet functions. The alternative minimization technique is then utilized to solve the final optimization problem. The subproblems for each individual variable are convex and their solutions have explicit expressions. Moreover, the computational complexity of the algorithm is discussed. Experimental results on both synthetic and real PolSAR data demonstrate the validity of the proposed algorithm.**

***Index Terms*—Nonconvex optimization, polarimetric synthetic aperture radar (PolSAR), variational method.**

I. Introduction

POLARIMETRIC synthetic aperture radar (PolSAR) can provide more information about the targets compared with single-channel SAR and PolSAR has wide applications in many fields. However, its coherent imaging mechanism causes serious speckle noise, which greatly affects the accuracy of classification of PolSAR data. So speckle reduction is particularly important for the successful applications of PolSAR.

In the past two decades, a variety of methods have been proposed for PolSAR data speckle suppression, including classical filtering techniques [1]–[4], nonlocal (NL) means filtering approaches [5]–[7], and variational methods [8], [9]. The classical filtering approaches include the refined Lee filter [1], the scattering model based filter [2], the intensity-driven adaptive-neighborhood filter [3], the model-based PolSAR filter [4]. This type of methods are most commonly used since they are fast and easy to use. However, they are spatial local filters, which may degrade the image spatial resolution and blur the targets concerned. The NL means filtering approaches include the pretest filter [5], the stochastic distance-based filter [6], and the NL-SAR filter [7]. This type of methods can well preserve the repetitive structures and give a better performance compared with the classical filters. However, these methods have patch-like artifacts due to the average of several pixel values that do not truly belong to the same underlying structure and present huge computational burden.

In recent years, variational methods have been widely studied for SAR image despeckling [10]–[13] since they can effectively reduce speckle without smearing the sharp edges. However, they are not suitable for PolSAR covariance data which are complex-valued and contaminated by a combination of multiplicative and additive noise [2]. In [14], an adaptive TV model was proposed to reduce speckle of the diagonal elements of covariance data. However, it ignores the off-diagonal elements, which leads to the loss of some important polarimetric information. To retain these information, a Wishart distribution and TV-based variational model (called WisTV) was proposed in [8] for the whole PolSAR covariance data despeckling. Furthermore, to preserve more details of PolSAR image, a NL TV-based variational model called WisNLTV was also proposed in [9], which gives a better performance but with higher computational complexity. However, the algorithms designed in [8], [9] do not take the positive definite (PD) constraint into account directly. Instead, they first solved the unconstrained optimization problem and then projected the solution onto the set of PD matrices. In addition, the parameters in the algorithms depend heavily on the data.

The purpose of this letter is to address the above two issues. First, a sigmoid function-based normalization method for the PolSAR covariance data is proposed, which can ensure that the parameters can be chosen uniformly for different data. Then, to guarantee the PD property, a new algorithm is designed to solve the WisTV problem according to the orthogonal decomposition of the PD variables and the equivalent representations of the trace and logdet functions. A main feature of the proposed algorithm is that each subproblem has a closed-form solution which makes the algorithm fast. Experimental results demonstrate the validity of the proposed algorithm.

II. New Algorithm for the WisTV Model

A. WisTV Model

For PolSAR data, speckle suppression should be carried out based on the whole covariance or coherence matrix, which contains

Manuscript received June 18, 2016; revised August 19, 2016; accepted August 21, 2016. Date of publication August 24, 2016; date of current version September 1, 2016. This work was supported in part by the National Natural Science Foundation of China under Grant 61379093, Grant 11131006, and Grant 61602483, in part by the Strategic Priority Research Program, in part by the CAS under Grant XDB02080003, in part by the BMST Grant D16110400140000 and Grant D161100001416001, and in part by the Early Career Development Award of SKLMCCS. The associate editor coordinating the review of this manuscript and approving it for publication was Prof. Qian He.

X. Nie is with the State Key Lab of Management and Control for Complex System, Institute of Automation, Chinese Academy of Sciences, Beijing 100190, China (e-mail: xiangli.nie@ia.ac.cn).

H. Qiao is with the State Key Lab of Management and Control for Complex System, Institute of Automation, Chinese Academy of Sciences, Beijing 100190, China, and also with CAS Centre for Excellence in Brain Science and Intelligence Technology, Shanghai 200031, China (e-mail: hong.qiao@ia.ac.cn).

B. Zhang is with State Key Laboratory of Scientific and Engineering Computing and Institute of Applied Mathematics, Academy of Mathematics and Systems Science, Chinese Academy of Sciences, Beijing 100190, China (e-mail: b.zhang@amt.ac.cn).

Y. Chen is with the Institute for Computer Graphics and Vision, Graz University of Technology, Graz A-8010, Austria (e-mail: chenyunjin_nudt@hotmail.com).

Color versions of one or more of the figures in this paper are available online at http://ieeexplore.ieee.org.

Digital Object Identifier 10.1109/LSP.2016.2602299

the second-order statistics [2]. In every resolution element, the covariance or coherence matrix is a 3×3 complex Hermitian matrix whose diagonal elements are real and characterized by multiplicative noise and whose off-diagonal elements are complex and characterized by a combination of multiplicative and additive noise [15].

For an area of size $m \times n$, the observed covariance data $\boldsymbol{Z}$ and the underlying noise-free covariance data $\boldsymbol{C}$ are fourth-order tensors with size $m \times n \times 3 \times 3$. In our previous paper [8], a complex Wishart distribution and TV based variational model, named WisTV, is proposed for PolSAR covariance data speckle reduction, which reads as follows:

$$\hat{\boldsymbol{C}} = \underset{C_i \in \boldsymbol{H}^3_{++}}{\operatorname{argmin}} \left\{ \lambda \sum_{i \in I} \left[\operatorname{Tr}(C_i^{-1} Z_i) + \log\det(C_i) \right] + \|\boldsymbol{C}\|_{\mathrm{TV}} \right\} \quad (1)$$

where $C_i := \boldsymbol{C}(i_1, i_2, :, :)$ and $Z_i := \boldsymbol{Z}(i_1, i_2, :, :)$ are 3×3 matrices with $I = \{i = (i_1, i_2) \mid 1 \le i_1 \le m, 1 \le i_2 \le n\}$, $\boldsymbol{H}^3_{++}$ denotes the set of 3×3 Hermitian PD matrices, λ is the regularization parameter, $\operatorname{Tr}(\cdot)$ and $\det(\cdot)$ denote the trace and the determinant of a matrix, respectively. Here, $\|\boldsymbol{C}\|_{TV}$ is the TV regularization term in the complex field defined as

$$\|\boldsymbol{C}\|_{TV} = \sum_{i \in I} \|\nabla C_i\|_F = \sum_{i \in I} \sqrt{\sum_{j \in J} (C^*_{ij_x} C_{ij_x} + C^*_{ij_y} C_{ij_y})} \quad (2)$$

where "∇" is the gradient operator, $C_{ij} := \boldsymbol{C}(i_1, i_2, j_1, j_2)$ with $J = \{j = (j_1, j_2) \,|\, 1 \le j_1 \le 3, 1 \le j_2 \le 3\}$, C_{ij_x} and C_{ij_y} are the first-order finite difference of the matrix $C_{.j} := \boldsymbol{C}(:, :, j_1, j_2)$ at pixel i in the horizontal and vertical directions, respectively, and the superscript "$*$" stands for the complex conjugate. As discussed in [8], the objective function in (1) is real-valued and nonconvex due to the concave property of log determinant.

B. PolSAR Covariance Data Normalization

The PolSAR covariance data from different PolSAR systems vary greatly, which makes it difficult to find uniform parameters in algorithms for different data. In addition, the dynamic ranges of the covariance data from the same PolSAR system also vary greatly, which would cause color smearing in the results obtained by the variational methods. However, the commonly used z-score and min–max normalization methods would change the statistical property of the covariance data and can not deal with the details-smearing problem. Therefore, we propose a sigmoid function-based normalization method in this section, which would preserve the Wishart distribution of the covariance data and, meanwhile, make the parameters to be chosen uniformly for different data.

Consider the sigmoid function $f_0(x) = 1/(1 + \exp(-x))$, whose range of values is from 0 to 1 for $x \in (-\infty, +\infty)$. Since the mean values of the diagonal elements of the covariance matrices are positive, the following transform is used to normalize the PolSAR data $f(x) = 2/(1 + \exp(-tx)) - 1$, where t is the weight controlling the slope. This function ranges from 0 to 1 for $x \in [0, +\infty)$. Specifically, let $M_1 = \boldsymbol{Z}(:, :, 1, 1)$, $M_2 = \boldsymbol{Z}(:, :, 2, 2)$, $M_3 = \boldsymbol{Z}(:, :, 3, 3)$, $N_1 = (M_1 + M_2 + M_3)/3$, and $u = \operatorname{mean}(N_1(:))$. Setting $f(u) = 0.5$ leads to $\hat{t} = \lceil \log(3)/u \rceil$ with $\lceil \cdot \rceil$ denoting the rounding up operator. Then, all the covariance data are normalized as follows:

$$\begin{aligned} N_2 &= 2/(1 + \exp(-\hat{t} N_1)) - 1, \\ \tilde{Z}_i &= Z_i N_2(i_1, i_2)/N_1(i_1, i_2),\ i = (i_1, i_2) \in I \end{aligned} \quad (3)$$

where $\tilde{\boldsymbol{Z}}$ represents the data after normalization. Thus, the mean value of the diagonal elements of $\tilde{Z}_i$ is scaled between 0 and 1. This normalization operation can ensure that $\tilde{Z}_i$ still follows the Wishart distribution and the model (1) is still applicable. The noise-free covariance data corresponding to $\tilde{\boldsymbol{Z}}$ is denoted as $\tilde{\boldsymbol{C}}$. After the solution $\hat{\tilde{\boldsymbol{C}}}$ of problem (1) has been obtained by the new algorithm proposed in the next section, all the covariance data are rescaled to their original ranges by

$$\hat{C}_i = \hat{\tilde{C}}_i N_1(i_1, i_2)/N_2(i_1, i_2),\ i = (i_1, i_2) \in I. \quad (4)$$

C. Proposed Algorithm for the WisTV Model

Since the unknown matrix $\tilde{C}_i$ is PD, we can rewrite $\tilde{C}_i$ as $\Phi_i \Phi_i^H + \delta E$, where the superscript "H" indicates the complex conjugate transpose, $\delta > 0$ is a small parameter to guarantee the PD property and E is an identity matrix. Thus, the original problem (1) with the positive definite constraint for $\tilde{\boldsymbol{C}}$ is transformed into the following unconstrained optimization problem for Φ:

$$\begin{aligned} \hat{\boldsymbol{\Phi}} = \underset{\Phi_i}{\operatorname{argmin}} \Bigg\{ & \lambda \sum_{i \in I} \left[\operatorname{Tr}((\Phi_i \Phi_i^H + \delta E)^{-1} Z_i) + \log\det(\Phi_i \Phi_i^H \right. \\ & \left. + \delta E) \right] + \sum_{i \in I} \|\nabla(\Phi_i \Phi_i^H + \delta E)\|_F \Bigg\}. \end{aligned} \quad (5)$$

By Proposition 3.1 in [16], the trace term can be transformed into a convex representation by using the Woodbury matrix identity

$$\begin{aligned} \operatorname{Tr}[(\Phi\Phi^H + \delta E)^{-1} Z] = \min_{\eta} \Bigg[\operatorname{Tr} \Bigg(& \frac{\mathrm{U}\mathrm{U}^H}{\delta} - \frac{U \eta^H \Phi^H}{\sqrt{\delta}} \\ & - \frac{U^H \Phi \eta}{\sqrt{\delta}} + \Phi \eta \eta^H \Phi^H + \delta \eta \eta^H \Bigg) \Bigg] \end{aligned} \quad (6)$$

where $\mathrm{U}\mathrm{U}^H = \tilde{Z}$ and η is an auxiliary variable. In addition, based on the singular value decomposition, we have $\det(\Phi\Phi^H + \delta E) = \det(\Phi^H \Phi + \delta E) + \mathrm{const}$. Furthermore, for a concave function, the conjugate function of its conjugate function is itself [16]. By Lemma 3 in [9], the log-determinant term is equivalent to the following representation:

$$\operatorname{logdet}(\Phi\Phi^H + \delta E) = \min_{\Psi \in \boldsymbol{H}^3_{++}} \left\{ \operatorname{Tr}[\Psi(\Phi^H \Phi + \delta E)] - \operatorname{logdet}(\Psi) \right\} \quad (7)$$

where Ψ is an auxiliary PD matrix.

Substituting (6) and (7) into (5) gives the optimization problem

$$\begin{aligned} \underset{\Psi_i \in \boldsymbol{H}^3_{++}, \eta_i, \Phi_i}{\operatorname{argmin}} \Bigg\{ & \lambda \sum_{i \in I} \Bigg[\operatorname{Tr} \Bigg(\frac{U_i U_i^H}{\delta} - \frac{U_i \eta_i^H \Phi_i^H}{\sqrt{\delta}} - \frac{U_i^H \Phi_i \eta_i}{\sqrt{\delta}} \\ & + \Phi_i \eta_i \eta_i^H \Phi_i^H + \delta \eta_i \eta_i^H \\ & + \Psi_i (\Phi_i^H \Phi_i + \delta E)) - \log\det(\Psi_i) \Big] \\ & + \sum_{i \in I} \|\nabla(\Phi_i \Phi_i^H + \delta E)\|_F \Bigg\}. \end{aligned} \quad (8)$$

We now use the alternative minimization technique to solve the above problem. To this end, letting the gradient of the objective function in (8) with respect to Ψ_i which is $\Phi_i^H \Phi_i + \delta E - \Psi_i^{-1}$ be

zero gives

$$\Psi_i = (\Phi_i^H \Phi_i + \delta E)^{-1}, \quad i \in I. \tag{9}$$

Let the gradient of the objective function in (8) with respect to η_i which is $-\Phi_i^H U_i/\sqrt{\delta} + \Phi_i^H \Phi_i \eta_i + \delta\eta_i$ be zero to get

$$\eta_i = \frac{1}{\sqrt{\delta}}(\Phi_i^H \Phi_i + \delta E)^{-1}\Phi_i^H U_i, \quad i \in I. \tag{10}$$

We use the first-order primal-dual algorithm [17], [11] to solve the Φ-subproblem. Before doing this, define

$$\mathrm{F}(\Phi) := \lambda \sum_{i\in I} \mathrm{Tr}\left[(\eta_i\eta_i^H + \Psi_i)\Phi_i^H\Phi_i - \frac{U_i\eta_i^H\Phi_i^H}{\sqrt{\delta}} - \frac{U_i^H\Phi_i\eta_i}{\sqrt{\delta}}\right].$$

Notice that $\|\tilde{\boldsymbol{C}}\|_{\mathrm{TV}} = \|\nabla\tilde{\boldsymbol{C}}\|_1 = \max_{\|\mathcal{P}\|_\infty \le 1} \langle \nabla\tilde{\boldsymbol{C}}, \mathcal{P}\rangle$, where $\mathcal{P}$ is the dual variable with size $m \times n \times 3 \times 3 \times 2$, $\langle\cdot,\cdot\rangle$ denotes the inner product, which is the sum of the products of the corresponding elements, and $\|\mathcal{P}\|_\infty$ denotes the discrete maximum norm defined as

$$\|\mathcal{P}\|_\infty = \max_{i\in I}|\mathcal{P}_i| = \max_{i\in I}\sqrt{\sum_{j\in J}[\mathcal{P}_{i,j,1}\mathcal{P}^*_{i,j,1} + \mathcal{P}_{i,j,2}\mathcal{P}^*_{i,j,2}]} \tag{11}$$

with $\mathcal{P}_i = \mathcal{P}(i_1, i_2, :, :, :)$ and $\mathcal{P}_{i,j,r} = \mathcal{P}(i_1, i_2, j_1, j_2, r)$, $r = \{1, 2\}$. In addition, the discrete divergence operator is defined as $\mathrm{div}\mathcal{P} = \mathcal{P}_x^1 + \mathcal{P}_y^2$ with $\mathcal{P}^r = \mathcal{P}(:, :, :, :, r)$ and $\mathcal{P}_x^1$ and $\mathcal{P}_y^2$ are the first-order difference in the horizontal and vertical directions. The divergence operator is adjoint to the discrete gradient operator, i.e., $\langle\nabla\tilde{\boldsymbol{C}}, \mathcal{P}\rangle = -\langle\tilde{\boldsymbol{C}}, \mathrm{div}\mathcal{P}\rangle$. The primal-dual formulation of the Φ-subproblem is

$$\operatorname*{argmin}_{\Phi_i}\operatorname*{argmax}_{\|\mathcal{P}\|_\infty\le 1}\left\{F(\Phi) - \langle\tilde{\boldsymbol{C}}, \mathrm{div}\mathcal{P}\rangle\right\}$$

where $\tilde{C}_i = \Phi_i\Phi_i^H + \delta E$. Thus, we obtain the following algorithm for the Φ-subproblem:

$$\mathcal{P}^{(k+1)} = \operatorname*{argmin}_{\|\mathcal{P}\|_\infty\le 1}\{-\langle\mathcal{P}, \nabla\bar{\boldsymbol{C}}^{(k)}\rangle + \rho\|\mathcal{P} - \mathcal{P}^{(k)}\|_F^2\} \tag{12}$$

$$\Phi^{(k+1)} = \operatorname*{argmin}_{\Phi_i}\{\mathrm{F}(\Phi) - \sum_{i\in I}[\langle\Phi_i\Phi_i^H, \mathrm{div}\mathcal{P}_i^{(k+1)}\rangle + \rho\|\Phi_i - \Phi_i^{(k)}\|_F^2]\} \tag{13}$$

$$\tilde{C}_i^{(k+1)} = \Phi_i^{(k+1)}{\Phi_i^{(k+1)}}^H + \delta E, \quad i \in I \tag{14}$$

$$\bar{\boldsymbol{C}}^{(k+1)} = 2\tilde{\boldsymbol{C}}^{(k+1)} - \tilde{\boldsymbol{C}}^{(k)}. \tag{15}$$

Note that problem (13) is with respect to variable Φ_i and the last summing term in (13) acts on Φ_i, which is an inertial term and controls the degree of variable Φ_i approaching $\Phi_i^{(k)}$. The solution of the $\mathcal{P}$-subproblem (12) is given by

$$\mathcal{P}^{(k+1)} = \mathcal{P}^{(k)} + \frac{1}{\rho}\nabla_w\bar{\boldsymbol{C}}^{(k)},\ \mathcal{P}_i^{(k+1)} = \frac{\mathcal{P}_i^{(k+1)}}{\max(|\mathcal{P}_i^{(k+1)}|, 1)}. \tag{16}$$

Letting the gradient of the objective function in (13) with respect to Φ_i, which is $\lambda\Phi_i(\eta_i\eta_i^H + \Psi_i) - \lambda U_i\eta_i^H/\sqrt{\delta} - \mathrm{div}\mathcal{P}_i^H\Phi_i + \rho(\Phi_i - \Phi_i^{(k)})$, be zero gives

$$\Phi_i(\lambda\eta_i\eta_i^H + \lambda\Psi_i + \rho E) - \mathrm{div}\mathcal{P}_i^H\Phi_i = \lambda U_i\eta_i^H/\sqrt{\delta} + \rho\Phi_i^{(k)}.$$

Algorithm 1: The WisTV-FRAM Algorithm.

1: **Input:** The observed covariance data $\boldsymbol{Z}$, λ, ρ, $\delta > 0$.
2: Normalize $\boldsymbol{Z}$ according to (3) to obtain $\tilde{\boldsymbol{Z}}$.
3: Initialize $U_i = \tilde{Z}_i^{1/2}$, $\Phi_i^{(1)} = U_i$, $\bar{\boldsymbol{C}}^{(1)} = \tilde{\boldsymbol{Z}}$, $\tilde{\boldsymbol{C}}^{(1)} = \tilde{\boldsymbol{Z}}$, $\tilde{\boldsymbol{C}}^{(0)} = \mathrm{zeros}(\mathrm{size}(\boldsymbol{Z}))$, $\mathcal{P}^{(1)} = \mathrm{zeros}(\mathrm{size}(\boldsymbol{Z}), 2)$.
4: **while** $k < 150$ and $\|\tilde{\boldsymbol{C}}^{(k)} - \tilde{\boldsymbol{C}}^{(k-1)}\|_F / \|\tilde{\boldsymbol{C}}^{(k-1)}\|_F < 0.001$ **do**
5: Compute Ψ_i and η_i according to (9) and (10).
6: Compute $\mathcal{P}$ and Φ_i according to (16) and (17).
7: Update $\tilde{\boldsymbol{C}}$ and $\bar{\boldsymbol{C}}$ based on (14) and (15).
8: **end while**
9: Rescale $\hat{\tilde{\boldsymbol{C}}} = \tilde{\boldsymbol{C}}^{(k+1)}$ according to (4) to obtain $\hat{\boldsymbol{C}}$.
10: **Output:** $\hat{\boldsymbol{C}}$.

Define

$$A := \lambda\eta_i\eta_i^H + \lambda\Psi_i + \rho E, \quad B := -\mathrm{div}\mathcal{P}_i^H,$$
$$D := \frac{\lambda U_i\eta_i^H}{\sqrt{\delta}} + \rho\Phi_i^{(k)}.$$

Then, we have $(A^T \otimes E + E \otimes B)\mathrm{vec}(\Phi_i) = \mathrm{vec}(D)$, where the superscript "T" indicates the vector transpose, "$\otimes$" indicates the Kronecker product and "vec" denotes the vectorization. The solution of the problem (13) is thus given by

$$\Phi_i = \mathrm{reshape}((A^T \otimes E + E \otimes B)^{-1}\mathrm{vec}(D), 3, 3),\ i \in I. \tag{17}$$

The detailed process of the proposed algorithm called WisTV-FRAM is presented in Algorithm 1. Parameter λ controls the degree of penalty, which is very important and influences the result greatly. We found that after data normalization, λ is less sensitive to the data sets. Therefore, cross validation on the simulated data is utilized to choose λ. Parameter ρ controls the convergence rate. By [17], we know that condition $\rho > \|\mathrm{div}\|/2$ ensures the convergence of the primal-dual algorithm and that $\|\mathrm{div}\| \le 2\sqrt{2}$. Therefore, the result is not sensitive to parameter ρ. Parameter δ is a very small and fixed constant to guarantee the PD property. For an observed area of size $m \times n$, the size of U_i, Ψ_i, η_i, and Φ_i is 3×3, the size of $\mathrm{div}\mathcal{P}$ and $\tilde{\boldsymbol{C}}$ is $m \times n \times 3 \times 3$, and the size of $\nabla\bar{\boldsymbol{C}}$ is $m \times n \times 3 \times 3 \times 2$. It is known that the inverse, the matrix–matrix product and the Kronecker product of 3×3 matrices need 3^3, 3^3, and 3^4 computational time, respectively. Thus, the total complexity of the proposed algorithm is $O(mnk)$ with k being the actual iterative number.

III. Experimental Results

This section evaluates the performance of the proposed method in comparison with three methods, the Refined Lee filter [1], the NL-SAR filter [7], and the WisTV method [8]. For the proposed algorithm, the parameters are set as follows: $\lambda = 0.005, \delta = 10^{-5}$, and $\rho = 2$. The despeckling results are evaluated by the visual Pauli decomposition image and the quantitative indicators discussed in [8], [18], including the equivalent number of looks (ENL), which measures the degree of speckle reduction and is computed in the chosen homogenous regions as marked by the white rectangle in Figs. 1(a)–2(a); the polarimetric information preservation indicators: the radiometric parameters (Ra), the complex correlation parameters (Ca, Cp), the Cloude–Pottier parameters (En, An, Al), and the co-polar (P_{co}) and cross-polar (P_{cr}) polarization signatures; and the edge-preservation degree indicator based on the ratio of average (EPD-ROA).

Figs. 1 and 2 present the visual comparison results on simulated and real PolSAR data, respectively. From Figs. 1 and 2, it can be

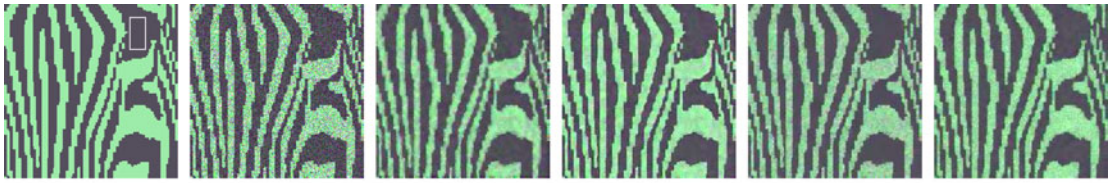

Fig. 1. Comparison results on simulated data (180×180). (a) Ground truth. (b) 3-look data. (c) Refined Lee. (d) NL-SAR. (e) WisTV. (f) WisTV-FRAM.

Fig. 2. Comparison results on real data (4-look, 350×350). (a) Original data. (b) Refined Lee. (c) NL-SAR. (d) WisTV. (e) WisTV-FRAM.

TABLE I
QUANTITATIVE EVALUATION ON THE SIMULATED POLSAR DATA

Methods/Indicators	Ra	Ca	Cp	En	An	Al	P_{co}	P_{cr}	ENL	EPD-HD	EPD-VD
Refined Lee	0.1120	0.3712	0.2501	0.0422	0.3123	0.0517	0.5951	0.5865	133.5124	0.9414	0.9898
NL-SAR	0.09612	0.3518	0.2981	**0.0365**	0.3096	0.0503	**0.5122**	**0.5201**	158.8203	**0.9901**	0.9927
WisTV	0.2044	**0.2871**	**0.1994**	0.1320	0.6159	0.0523	0.5355	0.5386	**162.2470**	0.9366	0.9941
WisTV-FRAM	**0.09036**	0.3897	0.2680	0.0572	**0.2598**	**0.0392**	0.5732	0.5683	120.5004	0.9432	**0.9943**

TABLE II
QUANTITATIVE EVALUATION ON REAL POLSAR DATA

Method	ENL			EPD-ROA					
	HH	HV	VV	HH-HD	HH-VD	HV-HD	HV-VD	VV-HD	VV-VD
Refined Lee	13.41	17.67	17.29	0.5975	0.7001	0.6043	0.7091	0.5885	0.7060
NL-SAR	15.23	23.18	20.42	0.6866	0.7698	0.6896	0.7769	0.6832	0.7705
WisTV	**25.92**	**63.08**	**40.56**	**0.6983**	0.7771	0.6901	0.7765	0.6891	0.7752
WisTV-FRAM	14.20	25.68	17.33	0.6923	**0.7806**	**0.7287**	**0.8106**	**0.6904**	**0.7810**

seen that the refined Lee filter degrades the spatial resolution and blurs the textures together with a pixellation effect in the flat area. The NL-SAR filter, as the state-of-the-art method, gives a better visual performance with the resolution and textures being well preserved. But, it may lead to patch-like effects in the uniform region. The WisTV approach gives inadequate despeckling results in the areas of higher pixel-values such as the green regions in Fig. 1(e) and oversmoothed results in the areas of lower pixel-values such as the coastal region in Fig. 2(d), due to the less effective data normalization method. In addition, the WisTV method blurs the textures in the center area and certain details in the sea area in Fig. 2(d). In contrast, the WisTV-FRAM method can well reduce speckle noise in the whole image and, meanwhile, well preserve the textures and details of the images.

Tables I and II present the quantitative evaluation results. It can be observed that the WisTV-FRAM method improves the values of the Cloude–Pottier parameters over WisTV since WisTV-FRAM automatically guarantees the PD property of the solution whilst WisTV manually makes the solution to satisfy this PD property by setting a positive lower bound of the eigenvalues of the solution matrix which are related to the En, An and, Al values. On the other hand, WisTV gives oversmoothed results in the uniform regions which lead to larger ENL values, while WisTV-FRAM obtains larger EPD-ROA values in most cases, which reflects a better performance in the edge preservation. The values of other indicators obtained by WisTV-FRAM are close to those given by NL-SAR, but the computation complexity of WisTV-FRAM is much lower than that of NL-SAR.

IV. CONCLUSION

This letter proposed a new algorithm to solve the nonconvex WisTV model for the whole PolSAR covariance data despeckling. A sigmoid function-based normalization method was first designed, so the parameters of the algorithm can be chosen uniformly for different PolSAR data sets. Then, using the orthogonal decomposition of the PD variables and the equivalent representations of the trace and logdet functions, the WisTV model with the PD constraint was transformed into an unconstrained multivariable optimization problem. Finally, the new algorithm was derived for solving the convex optimization subproblems, based on the alternative minimization technique, where the solution of each subproblem has an explicit expression. The computational complexity of the proposed algorithm was also discussed. Experimental results demonstrated that the proposed method is more effective and better preserves the Cloude–Pottier parameters, edges, and details with a low complexity than the previous algorithms compared.

REFERENCES

[1] J. -S. Lee, M. R. Grunes, and G. de Grandi, "Polarimetric SAR speckle filtering and its implication for classification," *IEEE Trans. Geosci. Remote Sens.*, vol. 37, no. 5, pp. 2363–2373, Oct. 1999.

[2] J. -S. Lee, M. R. Grunes, D. L. Schuler, E. Pottier, and L. Ferro-Famil, "Scattering-model-based speckle filtering of polarimetric SAR data," *IEEE Trans. Geosci. Remote Sens.*, vol. 44, no. 1, pp. 176–187, Jan. 2006.

[3] G. Vasile, E. Trouvé, J. -S. Lee, and V. Buzuloiu, "Intensity-driven adap tive-neighborhood technique for polarimetric and interferometric SAR parameters estimation," *IEEE Trans. Geosci. Remote Sens.*, vol. 44, no. 6, pp. 1609–1621, Jun. 2006.

[4] C. Lopez-Martinez and X. Fabregas, "Model-based polarimetric SAR speckle filter," *IEEE Trans. Geosci. Remote Sens.*, vol. 46, no. 11, pp. 3894–3907, Nov. 2008.

[5] J. Chen, Y. Chen, W. An, Y. Cui, and J. Yang, "Nonlocal filtering for polarimetric SAR data: A pretest approach," *IEEE Trans. Geosci. Remote Sens.*, vol. 49, no. 5, pp. 1744–1754, May 2011.

[6] L. Torres, S. J. Sant'Anna, C. da Costa Freitas, and A. C. Frery, "Speckle reduction in polarimetric SAR imagery with stochastic distances and non-local means," *Pattern Recognit.*, vol. 47, no. 1, pp. 141–157, 2014.

[7] C. -A. Deledalle, L. Denis, F. Tupin, A. Reigber, and M. Jäger, "NL-SAR: A unified non-local framework for resolution-preserving (Pol)(In) SAR denoising," *IEEE Trans. Geosci. Remote Sens.*, vol. 53, no. 4, pp. 2021–2038, Apr. 2015.

[8] X. Nie, H. Qiao, and B. Zhang, "A variational model for PolSAR data speckle reduction based on the Wishart distribution," *IEEE Trans. Image Process.*, vol. 24, no. 4, pp. 1209–1222, Apr. 2015.

[9] X. Nie, H. Qiao, B. Zhang, and X. Huang, "A nonlocal TV-based variational method for PolSAR data speckle reduction," *IEEE Trans. Image Process.*, vol. 25, no. 6, pp. 2620–2634, Jun. 2016.

[10] S. Yun and H. Woo, "A new multiplicative denoising variational model based on mth root transformation," *IEEE Trans. Image Process.*, vol. 21, no. 5, pp. 2523–2533, May 2012.

[11] Y. Huang, L. Moisan, M. Ng, and T. Zeng, "Multiplicative noise removal via a learned dictionary," *IEEE Trans. Image Process.*, vol. 21, no. 11, pp. 4534–4543, Nov. 2012.

[12] W. Feng, H. Lei, and Y. Gao, "Speckle reduction via higher order total variation approach," *IEEE Trans. Image Process.*, vol. 23, no. 4, pp. 1831–1843, Apr. 2014.

[13] Y. Chen, W. Feng, R. Ranftl, H. Qiao, and T. Pock, "A higher-order MRF based variational model for multiplicative noise reduction," *IEEE Signal Process. Lett.*, vol. 21, no. 11, pp. 1370–1374, Nov. 2014.

[14] H. Liu, F. Yan, J. Zhu, and F. Fang, "Adaptive vectorial total variation models for multi-channel synthetic aperture radar images despeckling with fast algorithms," *IET Image Process.*, vol. 7, no. 9, pp. 795–804, Dec. 2013.

[15] J.-S. Lee and E. Pottier, *Polarimetric Radar Imaging: From Basics to Applications*. Boca Raton, FL, USA: CRC press, 2009.

[16] K. Yu, W. Xu, and Y. Gong, "Deep learning with kernel regularization for visual recognition," in *Proc. Adv. Neural Inform. Process. Syst.*, 2008, pp. 1889–1896.

[17] A. Chambolle and T. Pock, "A first-order primal-dual algorithm for convex problems with applications to imaging," *J. Math. Imaging Vis.*, vol. 40, no. 1, pp. 120–145, 2011.

[18] S. Foucher and C. Lopez-Martinez, "Analysis, evaluation and comparison of polarimetric SAR speckle filtering techniques," *IEEE Trans. Image Process.*, vol. 23, no. 4, pp. 1260–1270, Apr. 2014.